

Oxidation and deprotonation of synthetic Fe^{II}–Fe^{III} (oxy)hydroxycarbonate Green Rust: An X-ray photoelectron study

M. Mullet*, Y. Guillemin, C. Ruby

Laboratoire de Chimie Physique et Microbiologie pour l'Environnement, Nancy I University, CNRS, UMR 7564, 405 Rue de Vandoeuvre, 54600 Villers-lès-Nancy, France

Received 4 July 2007; received in revised form 15 October 2007; accepted 30 October 2007
Available online 4 November 2007

Abstract

X-ray photoelectron spectroscopy (XPS) was used to investigate chemical bonding and distribution of iron and oxygen species at the surface of Green Rusts (GRs). GRs with variable composition, i.e. Fe_{6(1-x)}Fe_x^{III}O₁₂H_{2(7-3x)}}CO₃·3H₂O where the Fe^{III} molar fraction of the positively charged hydroxide sheets, $x = [\text{Fe(III)}]/[\text{Fe(total)}]$ belongs to [1/3, 1], were synthesised under an inert atmosphere. The broadened Fe(2p_{3/2}) spectra were fitted using Gupta and Sen multiplets peaks and additional satellite and surface features. The [Fe(III)]/[Fe(total)] surface atomic ratios closely agree with the x ratios expected from the bulk composition, which gives a high degree of confidence on the validity of the proposed fitting procedure. The valence band spectra are also reported and show dependencies on iron speciation. The O(1s) spectra revealed the presence of O²⁻, OH⁻ species and adsorbed water. The hydroxyl component decreases with increasing x values, i.e. with the amount of ferric iron, while the oxide component increases. This study provides direct spectroscopic evidence of the deprotonation of hydroxyl groups that occurs simultaneously with the oxidation of ferrous iron within the GR structure. © 2007 Elsevier Inc. All rights reserved.

Keywords: Green Rusts; Iron oxyhydroxide; Deprotonation; Oxidation; X-ray photoelectron spectroscopy

1. Introduction

Fe^{II}–Fe^{III} hydroxysalts Green Rust (GR) compounds belong to the layered double hydroxide (LDH) family and obey the general chemical formula [Fe_{6(1-x)}Fe_x^{III}(OH)₂]^{x+}·[(x/n)Aⁿ⁻mH₂O]^{x-} where Aⁿ⁻ is an intercalated anion, e.g. Cl⁻, SO₄²⁻, CO₃²⁻, and x is the Fe(III) molar fraction [Fe(III)]/[Fe(total)] of the positively charged hydroxide sheets. LDH minerals such as pyroaurite Mg₆^{II}Fe₂^{III}(OH)₁₂CO₃·4H₂O or hydrotalcite Mg₄^{II}Al₂^{III}(OH)₁₂CO₃·3H₂O were identified in natural environment for quite a long time [1,2]. However, fougérite (Strunz classification, 4FE.05), which is the mineral counterpart of synthetic GR compounds, was isolated from a hydromorphic soil more recently and characterised by Mössbauer, Raman and X-ray absorption spectroscopies during the period 1996–2000 [3–5].

LDH solid compounds are very often synthesised in the laboratory by the coprecipitation of controlled amount of M^{II} and M^{III} cations in aqueous solution [6,7]. One single solid state phase is generally obtained for M^{III} molar fraction x situated between 0.25 and 0.33. Its upper limit 0.33 corresponds to an ordered hexagonal pavement of M^{II}–M^{III} cations where each M^{III} cation is surrounded by 6 M^{II} cations [8]. The strong electrostatic repulsion among M^{III} cations was proposed to explain the quasi-absence of LDH having an x ratio higher than 0.33. More specifically, for Fe^{II}–Fe^{III} LDH compound synthesised in carbonated aqueous medium, the coprecipitation method performed at values of x higher than 0.33 leads to a mixture of magnetite Fe₃O₄ and “stoichiometric” hydroxycarbonate Green Rust GR(CO₃²⁻) of formula Fe₄^{II}Fe₂^{III}(OH)₁₂CO₃·3H₂O where $x = 0.33$ [9]. Moreover the fully ferric form GR(CO₃²⁻)* where $x = 1$ can be obtained by various pathways: (i) violent oxidation of a GR in aqueous solution [10,11], (ii) air oxidation of previously dried GR(CO₃²⁻) [11], (iii) air oxidation of GR(CO₃²⁻) in aqueous solution [11], (iv) electrochemical synthesis of thin GR layers [12]. Recent

*Corresponding author. Fax: +33 3 8327 5444.

E-mail address: martine.mullet@lcpme.cnrs-nancy.fr (M. Mullet).

studies demonstrated that a Fe^{II}–Fe^{III} solid solution exists between hydroxycarbonate GR(CO₃²⁻) ($x = 0.33$) and its fully ferric form GR(CO₃²⁻)* ($x = 1$) [13,14]. To take into account the required charge compensation, it was suggested that a deprotonation of the hydroxyl groups that surround the cations occurs simultaneously to the oxidation of Fe^{II} into Fe^{III} species corresponding to the chemical formula of GR(CO₃²⁻)*, i.e. Fe_{6(1-x)}^{II}Fe_{6x}^{III}O₁₂H_{2(7-3x)}CO₃ with $1/3 < x \leq 1$. Hansen and Koch [15] previously reported that the OH groups of the metal hydroxide layer of pyroaurite Mg₆Fe₂(OH)₁₆CO₃·3H₂O may be considered to have Bronsted acid/base properties using infrared spectroscopy. Although the deprotonation of the hydroxyl groups appears convincing, no direct evidence of this process is available yet.

There have been extensive studies devoted to the characterisation of the surface properties of iron oxides and (oxy)hydroxides using X-ray photoelectron spectroscopy (XPS). But no attempt was made to investigate the surface chemistry of synthetic GR compounds till now. XPS provides direct information on the elements present, their chemical state and their distribution. In addition, chemical reactions changing the chemical state of particular atoms are investigated from intensity variations and chemical shifts of the photoelectron spectra.

This paper aims to demonstrate that XPS is a well suitable technique to investigate the surface chemistry of GR hydroxysalts. However, GRs get easily oxidised in atmospheric conditions and surface analysis needs careful handling. The oxidation state of iron in GR(CO₃²⁻) lies between a Fe^{II}-rich Fe^{II}–Fe^{III} compound, i.e. GR(CO₃²⁻) at $x = 1/3$, and the fully oxidised Fe^{III} compound, i.e. GR(CO₃²⁻)* at $x = 1$, thus making this compound a good candidate to investigate the complex fitting procedure of iron. In fact, Fe(2p_{3/2}) spectra of GRs are broad, displaying multiplet peaks as well as satellite and surface features that probably explains the lack of literature data till now. The procedure reported by Grosvenor et al. [16] for a wide range of iron compounds is used in the present study. For the first time, the fitting of the Fe(2p_{3/2}) spectrum of stoichiometric Fe^{II}-rich GR is reported. Moreover, XPS analysis provides the first spectroscopic evidence that the oxidation of Fe(II) into Fe(III) in the GR structure is effectively accompanied by the deprotonation of the hydroxyl groups.

2. Experimental methods

2.1. Synthesis of stoichiometric hydroxycarbonate GR(CO₃²⁻)

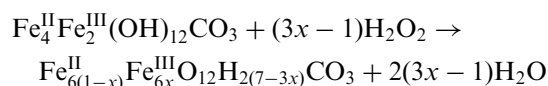
The synthesis of stoichiometric GR(CO₃²⁻) was carried out under a nitrogen circulation to minimise the amount of dissolved oxygen in the reactor. Appropriate amounts of FeSO₄·7H₂O, Fe₂(SO₄)₃·5H₂O and Na₂HPO₄ salts were dissolved in 200 mL of ion-exchanged water (Milli-Q, 18.2 MΩ cm⁻¹ resistivity) to give final concentrations

[Fe(total)] = 0.4 M with $x = [\text{Fe(III)}]/[\text{Fe(total)}] = 0.33$ and [PO₄³⁻] = 2 × 10⁻² M. Phosphate anion was added to stabilise the GR(CO₃²⁻) structure as previously discussed [17]. 20 mL of the Fe(II)–Fe(III) solution were then introduced in a glass reactor and the solution was deoxygenised under a nitrogen circulation during 30 min. After this period, 20 mL of a solution consisting of sodium carbonate ([CO₃²⁻] = 0.47 M) and sodium hydroxide ([OH⁻] = 0.8 M) was added in one drop in the reactor, the ratio of {*n*_{NaOH}/*n*_{Fe(total)}} being fixed at 2. The GR(CO₃²⁻) precipitated immediately, as evidenced by the characteristic bluish-green colour developed in the reactor. Replicates of stoichiometric hydroxycarbonate GR(CO₃²⁻) were synthesised simultaneously in five separate reactors in order to prepare the oxyhydroxycarbonate samples with five different compositions as described in the next section.

2.2. Preparation of GR(CO₃²⁻)* with variable composition

Oxyhydroxycarbonate GR(CO₃²⁻)* samples with different compositions were obtained by fast oxidation of stoichiometric hydroxycarbonate GR(CO₃²⁻) by hydrogen peroxide [13,14]. A 9.804 M H₂O₂ stock solution was added to the GR(CO₃²⁻) suspensions in one drop under vigorous stirring at 750 rpm and at a targeted molar ratio $n(\text{H}_2\text{O}_2)/n(\text{Fe}_{\text{total}})$:

- For $n(\text{H}_2\text{O}_2)/n(\text{Fe}_{\text{total}}) < 0.33$ the GR(CO₃²⁻) gets partially oxidised ($x < 1$) according to the following equation:



- For $n(\text{H}_2\text{O}_2)/n(\text{Fe}_{\text{total}}) \geq 0.33$, all Fe(II) of stoichiometric GR(CO₃²⁻) gets oxidised to yield the “fully ferric green Rust” GR(CO₃²⁻)* at $x = 1$ according to:



Therefore, appropriate amounts of H₂O₂, i.e., $n(\text{H}_2\text{O}_2)/n(\text{Fe}_{\text{total}}) = (3x - 1)/6$ were added to the five reactors to reach x values of 0.33, 0.50, 0.66, 0.87 and 1. The colour of the precipitates changes gradually upon H₂O₂ addition, from “bluish-green” ($x = 0.33$) to fully “brown-orange” ($x = 1$) thus reflecting increasing oxidation of Fe(II).

After a few minutes, the reactors were introduced inside a glovebox, the solid phases were filtered, washed with distilled and deoxygenated water and dried under an argon atmosphere for about 12 h. Owing to the instability of GRs, except for $x = 1$, analyses were carried out immediately after drying.

2.3. Characterisation of GRs minerals by (XPS)

XPS spectra were obtained using a KRATOS Axis Ultra X-ray photoelectron spectrometer with a monochromatised AlK α X-ray ($h\nu = 1486.6$ eV) operated at 150 W and a charge neutraliser. The samples were pressed onto a Cu tape inside the glovebox and transferred into the spectrometer through a second small glovebox mounted on the preparation chamber. The base pressure in the analytical chamber was $\approx 10^{-9}$ mbar. Spectra were collected at normal (90°) take-off angle. Survey scans were used to

determine the chemical elements at the GRs surface. They were acquired with an analyser pass energy of 160 eV and a sample analysis area of 0.3 mm \times 0.7 mm. Narrow region electron spectra were used to determine chemical state information. They were acquired with an analyser pass energy of 20 eV (instrumental resolution better than 0.5 eV) and a sample analysis area of 0.3 mm \times 0.7 mm. Sample charging effects on the measured binding energy positions were corrected by setting the lowest binding energy component of the C1s spectral envelope to 284.6 eV, i.e. the value generally accepted for adventitious carbon

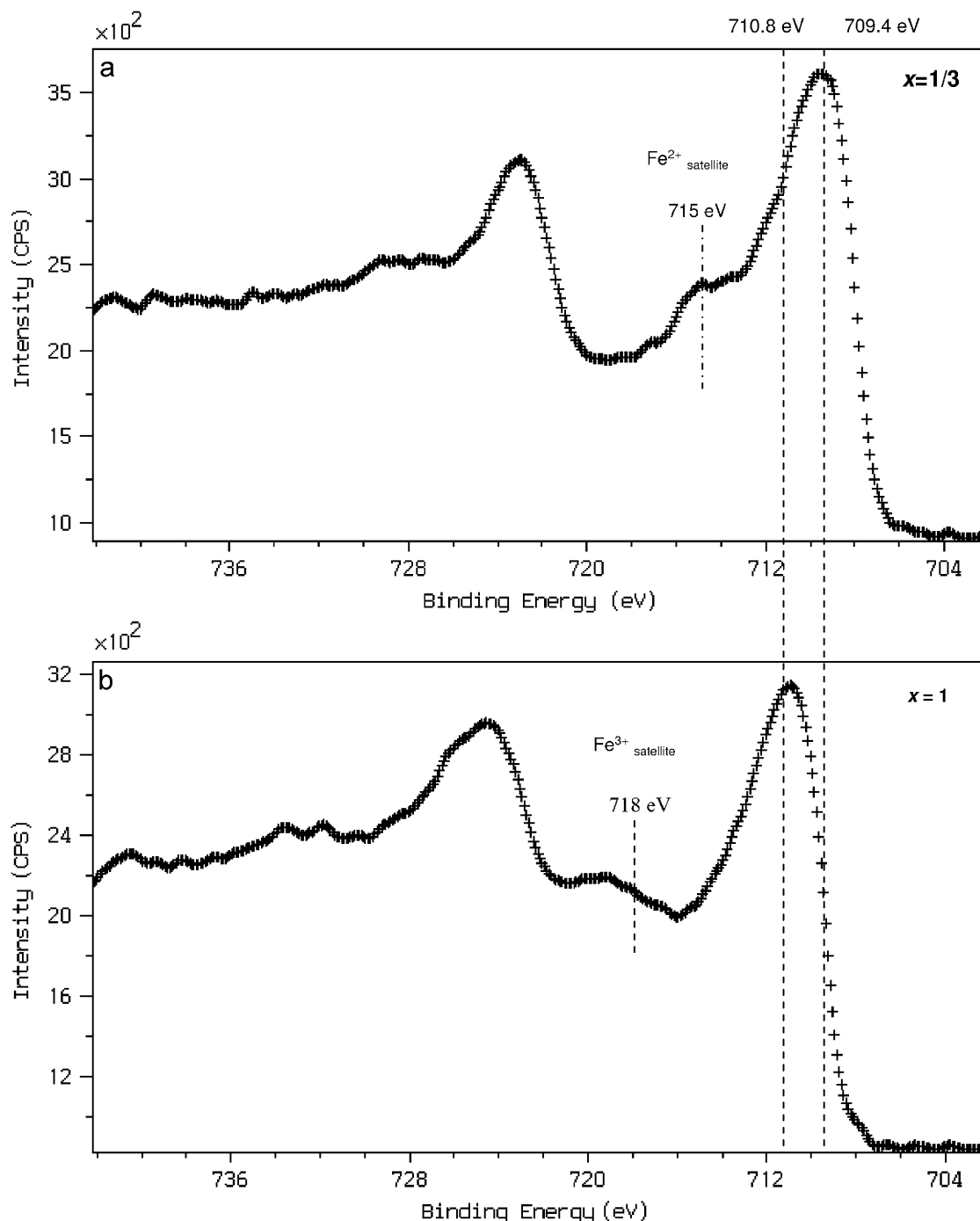


Fig. 1. Fe(2p) spectra of (a) stoichiometric GR(CO₃²⁻) (i.e. $x = 1/3$) and (b) fully ferric GR(CO₃²⁻)* (i.e. $x = 1$).

surface contamination. Spectra for iron and oxygen were fitted using a Shirley background and a Gaussian G (70%) Lorentzian L (30%) peak model.

3. Results

The survey spectra indicated the presence of Fe, O and C and minor amounts of residual sodium and phosphorus (~1%) at the surface of the GR samples. The carbon originated from both the presence of carbonate in the GRs structure and some adventitious carbon. The iron to oxygen ratios determined from broadscans utilising peak areas and sensitivity factors are close to 0.4 in agreement with the composition of GRs.

3.1. $Fe(2p_{3/2})$ spectrum

Broad $Fe(2p)$ spectra of stoichiometric $GR(CO_3^{2-})$ (i.e. $x = 1/3$) and fully ferric $GR(CO_3^{2-})^*$ (i.e. $x = 1$) are shown in Fig. 1. Broadening is attributed to multiplet splitting and shake-up phenomena. The main differences between the two spectra are the binding energies of peak maxima and the satellite features. In fact, spectra obtained for $x = 1/3$ (Fig. 1a) and $x = 1$ (Fig. 1b) clearly display peak maxima at ~709.4 and ~710.8 eV, respectively. The shift towards higher binding energy observed for ferric $GR(CO_3^{2-})$ is primarily attributed to the removal of Fe(II) into the GR(s) structure. Additionally, characteristic Fe^{2+} and Fe^{3+} satellite peaks are observed at ~715 and ~718 eV for $x = 1/3$ (Fig. 1a) and $x = 1$ (Fig. 1b), respectively [16].

To obtain further insight into the iron speciation in GRs with variable iron composition, fitting the spectra is required. To our knowledge, no data for Fe^{II} – Fe^{III} GR have been published yet. Fitting procedures of $Fe(2p)$ region spectra of iron (oxyhydr)oxides are usually complex including multiplet contributions and satellite features [18]. The complexity is enhanced in mixed valence compounds, those including overlapping multiplet peaks of Fe(II) and Fe(III) species. Grosvenor et al. [16] have shown that the $Fe(2p_{3/2})$ peak from a range of Fe(II) and Fe(III) high spin compounds can be well fitted using multiplets calculated by Gupta and Sen [19] and additional high binding energy surface and $2p_{3/2}$ satellite peaks. Note that the Gupta and Sen calculations take into account electrostatic interactions and spin–orbit coupling between the $2p$ core hole and the unpaired $3d$ electrons of the photoionised Fe cations. In particular, the procedure reported by Grosvenor et al. [16] was successfully used for fitting the complex $Fe(2p_{3/2})$ spectrum of Fe_3O_4 where both Fe(II) and Fe(III) species are present. The multiplet peak with lowest binding energy is located at 708.3 and 710.0 eV for Fe(II) and Fe(III) in Fe_3O_4 respectively and peak areas ratios relative to the main multiplet peak are 1.04 and 0.37 for Fe(II) and 0.91, 0.65 and 0.31 for Fe(III). These parameters were therefore employed as an initial estimate for fitting the spectra of GRs. Spectra of GRs were thus fitted by using Gupta and Sen closely spaced multiplet peaks for Fe(II) and Fe(III)

species, the multiplet peaks of the major Fe(II) or Fe(III) peak being constrained to the same shape, width and energy separation. A peak reporting to surface structures that exhibit different binding energies comparing to those located within the bulk was added with a higher binding energy than the multiplets. Low-intensity peaks from the bulk not well described by the Gupta and Sen multiplet peaks were previously suggested to be one possible cause of this surface peak. This high binding energy peak may be also ascribed to a decrease in the crystal field energy of the Fe ions located at the surface compared with those found within the bulk. The multiple reasons for the presence of this surface peak have been discussed in details in Grosvenor et al. [16]. To fill the rest of the envelope, single large peaks representing Fe(III) and Fe(II) satellite peaks were also added. The $Fe(2p_{3/2})$ spectra of fully oxidised $GR(CO_3^{2-})^*$ ($x = 1$) and GRs of variable composition are shown in Figs. 2 and 3 respectively and the multiplet peak parameters used to fit the spectra are listed in Table 1. The $Fe(2p_{3/2})$ peak of fully ferric $GR(CO_3^{2-})^*$ ($x = 1$) (Fig. 2) is well fitted using the four predicted Gupta and Sen multiplet peaks, a high binding energy surface structure at ~714.5 eV and a characteristic Fe(III) satellite peak at ~718 eV. Both binding energies of the multiplets and peak intensity ratios are close to those reported previously by Grosvenor et al. [16] to fit the Fe(III) component in Fe_3O_4 spectrum (Table 1). The $Fe(2p_{3/2})$ spectra of GRs of variable composition ($x = 0.33, 0.5$ and 0.87) (Fig. 3) were fitted by taking into account for the presence of Fe(II) in addition to Fe(III) species. Three Fe(II) multiplet peaks

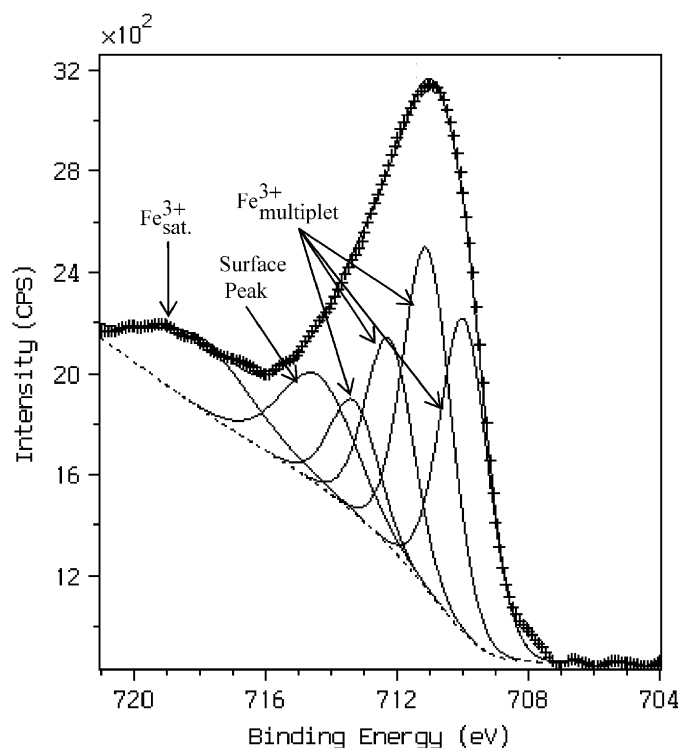


Fig. 2. $Fe(2p_{3/2})$ spectrum of fully oxidised $GR(CO_3^{2-})^*$ ($x = 1$).

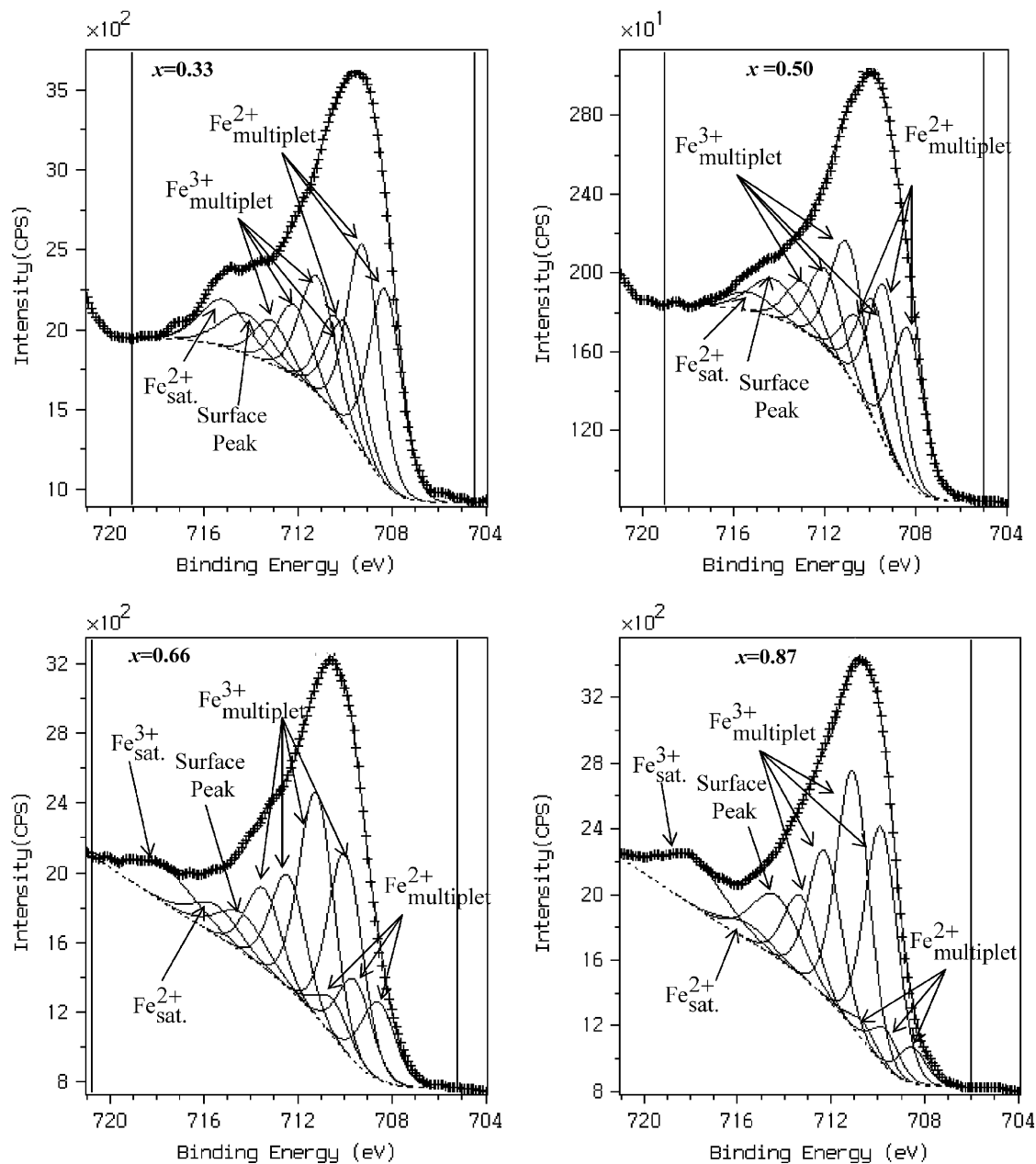


Fig. 3. Fe($2p_{3/2}$) spectra of GRs with variable composition ($x = 0.33, 0.50, 0.66,$ and 0.87).

(Table 1) and a broad Fe(II) satellite located at ~ 715 eV were used to fit these spectra. Although the presence of overlapping multiplets made it difficult to separate Fe(II) and Fe(III) species, the Fe(III) to Fe(total) surface atomic ratios, are fairly close to the x values calculated from the GR bulk composition (Table 1). The agreement between these values evidences that the fitting procedure used by Grosvenor et al. [16] is well suitable for GR compounds. Note that Fe(III) to Fe(total) surface atomic ratios are always slightly higher than those expected from the bulk composition. The higher amount of Fe(III) at the sample surface may be explained by some fortuitous oxidation of Fe(II) during sample handling despite the great care taken to preserve the surface from oxidation (Table 1).

3.2. O(1s) spectrum

The O(1s) photoelectron spectra of stoichiometric GR(CO_3^{2-}) (i.e. $x = 0.33$) and GR(CO_3^{2-})* of variable composition are illustrated in Figs. 4 and 5. All spectra are best fitted with peaks at ~ 529.4 , ~ 531 and ~ 532.9 eV corresponding to oxide oxygen, hydroxyl groups and adsorbed water respectively (Table 2) in agreement with previous studies [20,21]. The shape of the spectra clearly depends on the GRs composition, the oxide and hydroxyl components being increased and decreased with increasing x value, respectively. The spectra clearly evidence the deprotonation of hydroxyl groups that occur with increasing oxidising conditions.

Table 1
Gupta and Sen multiplet peaks parameters used to fit Fe(2p_{3/2}) spectra of GRs with variable composition

Bulk composition	Peak 1 (eV) (FWHM)	%	Peak 2 (eV) (FWHM)	%	Peak 3 (eV) (FWHM)	%	Peak 4 (eV) (FWHM)	%	(Fe(III))/(Fe(total)) surface ratio
$x = 0.33$									
Fe ²⁺	708.3 (1.6)	19.7	709.2 (1.6)	21.1	710.4 (1.6)	9.9	–	–	0.42
Fe ³⁺	710.0 (1.7)	11.2	711.2 (1.7)	12.6	712.2 (1.7)	7.7	713.2 (1.7)	4.7	
$x = 0.50$									
Fe ²⁺	708.4 (1.6)	17.7	709.4 (1.6)	18.2	710.5 (1.6)	8.54	–	–	0.51
Fe ³⁺	709.8 (1.7)	14.8	711.0 (1.7)	16.2	712.0 (1.7)	9.62	713.0 (1.7)	6.0	
$x = 0.66$									
Fe ²⁺	708.4 (1.6)	6.8	709.4 (1.6)	7.0	710.3 (1.6)	3.2	–	–	0.79
Fe ³⁺	709.9 (1.6)	20.7	711.1 (1.6)	22.7	712.2 (1.6)	13.3	713.3 (1.6)	7.7	
$x = 0.87$									
Fe ²⁺	708.5 (1.4)	3.0	709.7 (1.4)	3.1	710.6 (1.4)	1.5	–	–	0.90
Fe ³⁺	709.9 (1.6)	23.5	711.1 (1.6)	25.7	712.3 (1.6)	14.6	713.3 (1.6)	8.4	
$x = 1$									
Fe ³⁺	710.0 (1.7)	23.8	711.1 (1.7)	25.9	712.2 (1.7)	15.8	713.3 (1.7)	8.5	1

FWHM: Full-width at half-maximum.

Table 2
Binding energy values, FWHM (full-width at half-maximum), peak areas and interpretation for O(1s) spectra of GRs with variable composition

Bulk composition	O(1s) (FWHM) (eV)	Area %	Species
$x = 0.33$	529.4 (1.1)	10.5	O ²⁻
	531.0 (1.6)	82.5	OH ⁻
	533.0 (1.7)	7	H ₂ O
$x = 0.50$	529.4 (1.2)	21.3	O ²⁻
	531.1 (1.7)	71.2	OH ⁻
	533.1 (1.6)	7.5	H ₂ O
$x = 0.66$	529.4 (1.2)	33	O ²⁻
	531.0 (1.7)	64.5	OH ⁻
	533.0 (1.7)	2.5	H ₂ O
$x = 0.87$	529.5 (1.1)	36.5	O ²⁻
	530.9(1.6)	61.5	OH ⁻
	532.9(1.4)	1.9	H ₂ O
$x = 1$	529.5 (1.1)	32.7	O ²⁻
	531.0 (1.6)	63.1	OH ⁻
	532.8 (1.7)	4.2	H ₂ O

3.3. Valence band regions

The valence band region for stoichiometric GR(CO₃²⁻) ($x=0.33$) and fully ferric GR(CO₃²⁻)^{*} ($x=1$) are reported in Fig. 6. Temesghen and Sherwood [20] have interpreted the valence band spectra of iron and iron oxides by cluster and band structure calculations. The aim here is not to perform any calculations, but to show that useful information can be obtained from valence band region and that this could assist in the analysis of core levels for further studies of GRs. In fact, signatures of the two GRs are clearly different. The O(2s) region shows two peaks located at around 23 eV ($x = 0.33$) and 22 eV ($x = 1$). The shift towards lower binding energies for $x = 1$ agrees well

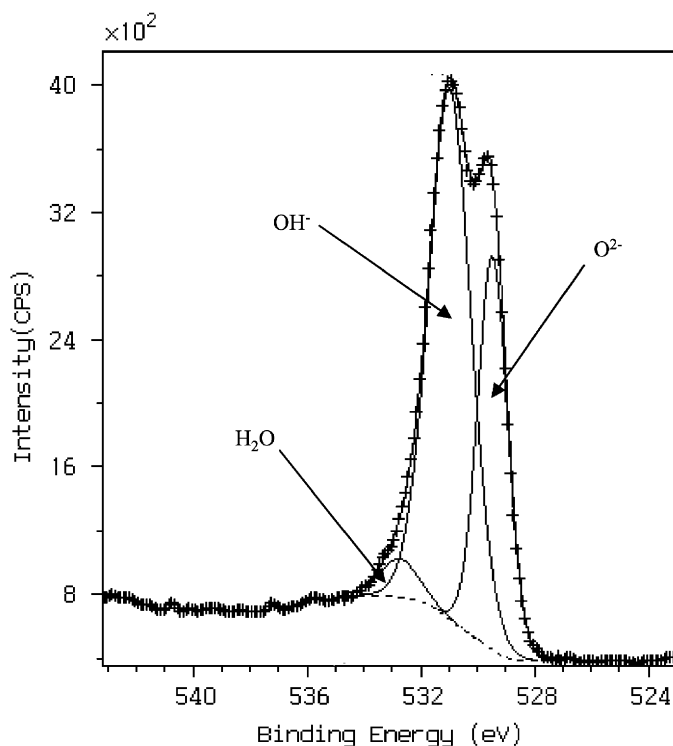


Fig. 4. O(1s) spectrum of fully oxidised GR(CO₃²⁻)^{*} ($x = 1$).

with the increase in the oxide component as previously discussed for the O(1s) core level. The feature observed at a binding energy of around 9.8 eV for stoichiometric GR ($x = 0.33$), is carefully assigned to emission from O(2p) orbital and may reflect the signature of hydroxyl groups (Table 1). Further investigation is required to well understand the origin of this peak. Another interesting aspect of the spectra is that the valence band region also displays two peak maxima located at around 4.2 and 5.8 eV, depending on the GR composition. The shift towards higher binding

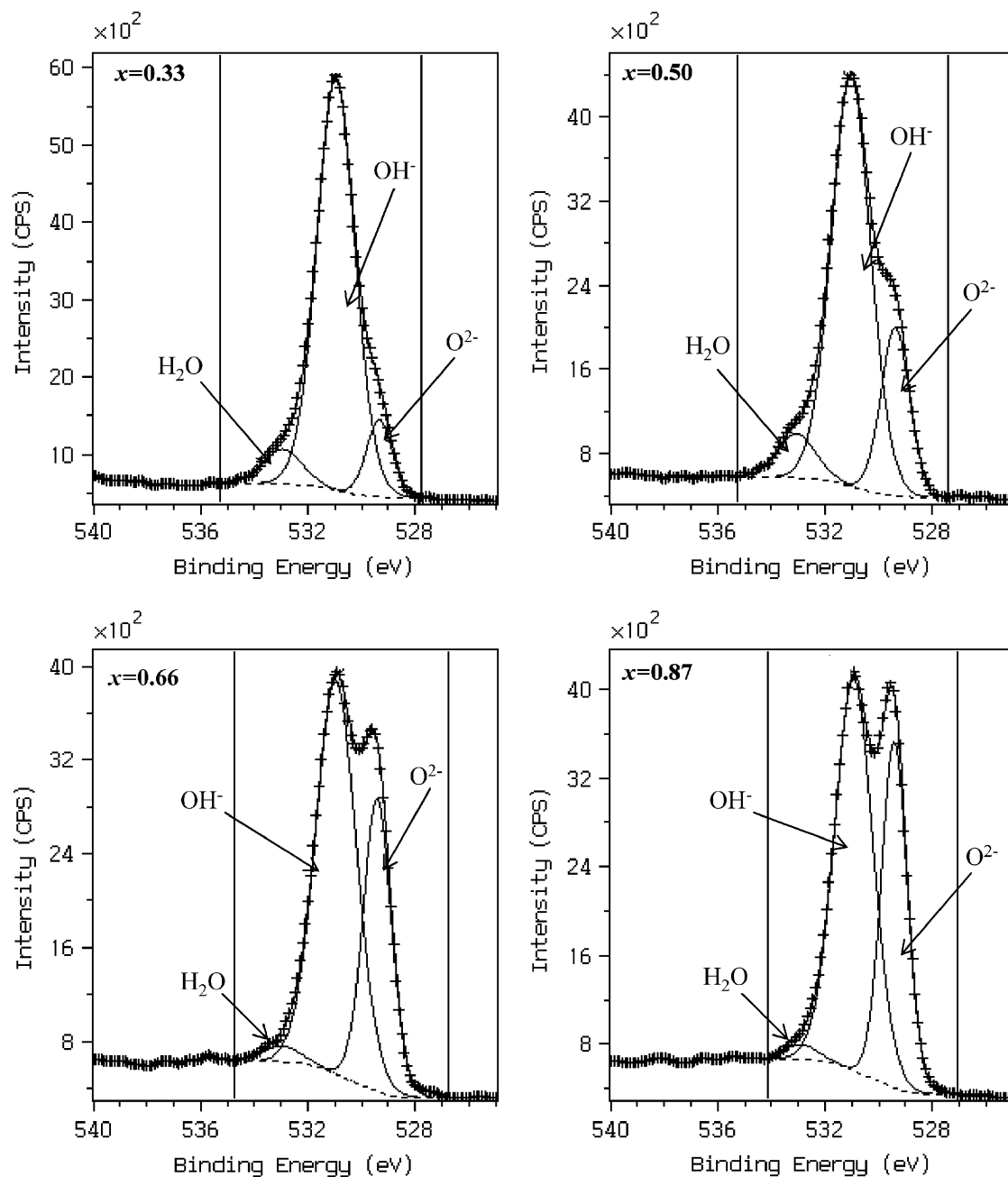


Fig. 5. O(1s) spectra of GRs with variable composition ($x = 0.33, 0.50, 0.66,$ and 0.87).

energy observed for $x = 1$ is due to the increasing amount of Fe(III) in agreement with the Fe($2p_{3/2}$) core level interpretation. The characteristic Fe(II) feature located at 4eV has been previously observed in the valence band spectrum of FeO [22]. In addition, the valence band spectrum of FeO displays a peak located at around 1.2 eV. The peak located at around 0.5 eV in the valence band spectrum of stoichiometric GR ($x = 0.33$) (Fig. 6), is probably characteristic of the presence of Fe(II) although it arises at a slightly lower binding energy. In fact, the intensity of this peak decreases with increasing x values (not shown) and is removed in the spectrum of fully ferric GR(CO_3^{2-})*. In spite some features are not definitively

identified in Fig. 6, it is clear from this first analysis, that the valence band region can also be used as a fingerprint to discriminate between the various composition of GRs.

4. Discussion

4.1. XPS GRs characterisation

A detailed surface analysis using XPS has been carried out for the first time on Green Rusts compounds. To the best of our knowledge, only spectra of fully ferric GR(CO_3^{2-})* have been reported until now and no attempt was made to fit the spectra [23,24]. The failure to analyse

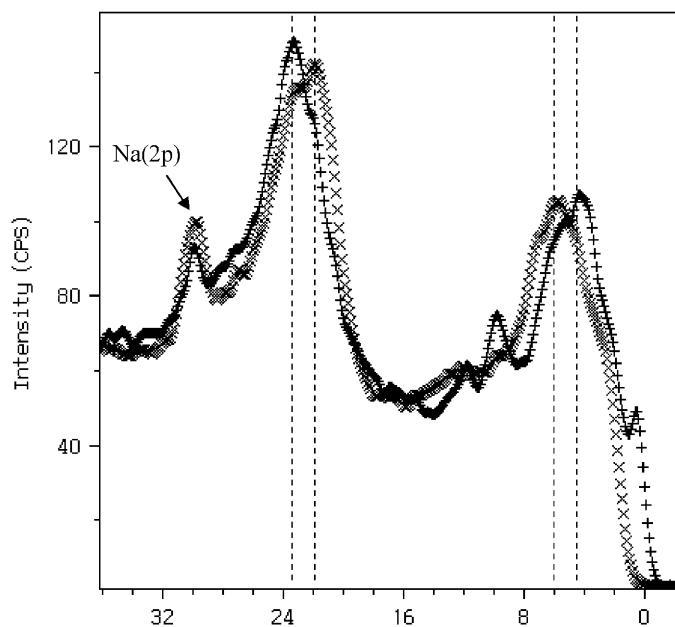


Fig. 6. Valence band XPS spectra of GRs: +: $x = 0.33$; x: $x = 1$.

GRs is partially explained by the high reactivity of these compounds towards oxygen. In fact, because XPS is only sensitive to the first atomic layers (~ 5 nm), great care is required to preserve the surface from oxidation. An experimental device that allows the synthesis of stoichiometric $\text{GR}(\text{CO}_3^{2-})$ ($x = 0.33$) and its subsequent oxidation into $\text{GR}(\text{CO}_3^{2-})^*$ with various compositions ($x = 0.50, 0.66, 0.87$ and 1), under an argon atmosphere, was considered for the present study. In addition to the high reactivity of GR compounds, the lack of XPS data originates from the complex analysis of the $\text{Fe}(2p)$ region that involves contributions from both $\text{Fe}(\text{II})$ and $\text{Fe}(\text{III})$ species. Only small differences in binding energies are observed between $\text{Fe}(\text{II})$ and $\text{Fe}(\text{III})$ bonded to oxygen and the spectral analysis is complicated by broad features and satellite structures. Nevertheless, the procedure reported by Grosvenor et al. [16] to fit the spectra of a range of iron oxides and in particular the multivalent Fe_3O_4 is well suitable for GRs compounds. $\text{Fe}(2p_{3/2})$ spectra of GR compounds can thus be well fitted using appropriate Gupta and Sen multiplets, high binding energy surface and $2p_{3/2}$ satellite peaks. Good agreement between the $[\text{Fe}(\text{III})]/[\text{Fe}(\text{total})]$ surface atomic ratios and x bulk values makes the fitting procedure reliable. The fitting procedure of the $\text{O}(1s)$ spectra of GR compounds is unambiguous, those clearly displaying expected features due to oxide (O^{2-}) and hydroxide (OH^-) as previously reported for other iron oxyhydroxides.

4.2. Oxidation pathway of $\text{Fe}^{\text{II}}\text{--Fe}^{\text{III}}$ hydroxycarbonate Green Rust compound

The investigation of the oxidation pathway of stoichiometric $\text{GR}(\text{CO}_3^{2-})$ ($x = 0.33$) to the fully ferric form at $x = 1$ has been previously carried out by using TEM, XRD, FTIR

and Mössbauer spectroscopies [13,14]. Refait et al. [10] and Legrand et al. [11] reported a solid state oxidation pathway involving the oxidation of $\text{Fe}(\text{II})$ into $\text{Fe}(\text{III})$ inside the crystal lattice. XRD diffraction patterns of the oxidised $\text{GR}(\text{CO}_3^{2-})^*$ were close to that of the initial product, showing a broadening of the diffraction lines and a small contraction of the unit cell due to the oxidation of $\text{Fe}(\text{II})$. The same behaviour was also reported by Ruby et al. [13] for GRs with variable compositions ($x = 0.33, 0.50$ and $x = 1$). Mössbauer spectroscopy was demonstrated to be a powerful tool to investigate the bulk oxidation state as well as the structural and magnetic properties of iron compounds. Mössbauer spectra of GRs evidenced the redox-flexibility of $\text{Fe}^{\text{II}}\text{--Fe}^{\text{III}}$ oxyhydroxycarbonate, $\text{Fe}_{6(1-x)}^{\text{II}}\text{Fe}_{6x}^{\text{III}}\text{O}_{(x-1/3)}\text{O}_{12}\text{H}_{2(7-3x)}\text{CO}_3$ where $x = [\text{Fe}(\text{III})]/[\text{Fe}(\text{total})]$ ranges between $1/3$ and 1 [13,14]. To satisfy the electrical neutrality of the GR structure, charge compensation is required. According to Legrand et al. [11], the charge compensation by CO_3^{2-} can be ruled out since the number of interlayer sites required is higher than those available. Additionally, these authors were able to demonstrate that the carbonate content into both $\text{GR}(\text{CO}_3^{2-})$ and ferric $\text{GR}(\text{CO}_3^{2-})^*$ was equivalent, meaning that the excess of positive charge induced by the oxidation process was not compensated by any excess of carbonate species in the interlayer. Legrand et al. [11] assume that the solid state oxidation process is associated to a deprotonation of the water molecules within the interlayers or at the $\text{Fe}(\text{O}, \text{H})$ octahedral sites in the layers. The second hypothesis, i.e. deprotonation of OH^- , is in good agreement with the evolution of the $\text{O}(1s)$ peak displayed in Fig. 5. The deprotonation affects rather the octahedrally coordinated hydroxyl species present in the brucite like sheets of GR. Indeed, these species are the nearest neighbours ligands of the Fe species and can more directly compensate the excess of positive charge induced by the oxidation of the $\text{Fe}(\text{II})$ into $\text{Fe}(\text{III})$ species. Therefore, the XPS results are in good agreement with the structural model proposed recently by Génin et al. [14] who pointed out that the deprotonation of OH^- occurs at the apexes of the octahedrons surrounding the Fe cations. Nevertheless, there was no direct evidence of the deprotonation of hydroxyl groups in these previous studies. This study provides firm spectroscopic evidence that the charge compensation does occur through the deprotonation of hydroxyls groups. Among the different Fe containing oxides and (oxyhydr)oxides, the deprotonation effect of $\text{GR}(\text{CO}_3^{2-})$ is unique and processes involving redox cycling of GRs in situ without dissolution–recrystallisation may occur [11,13]. Moreover, GRs are a pool of reductants for toxic metals species such as chromate [25] or inorganic oxyanions such as nitrate [7,26]. Of course, such processes involve the mineral surface and XPS appears as a powerful tool to investigate the surface reactions of GR compounds.

5. Conclusions

In summary, we evidenced that XPS is a powerful tool to investigate the surface chemistry of GR compounds.

The fitting of the Fe($2p_{3/2}$) spectra allowed to determine the Fe(III)/Fe(total) ratio during the progressive oxidation of Fe(II)-rich GR(CO₃²⁻) compound into fully ferric GR(CO₃²⁻)* compound. Additionally, first direct spectroscopic evidence of the deprotonation of hydroxyl groups occurring simultaneously to the oxidation of ferrous species is provided from the O(1s) spectra analysis.

Acknowledgments

The authors acknowledge J. Lambert from the Laboratoire de Chimie Physique et Microbiologie pour l'Environnement for the XPS analyses. We are grateful to Dr. J.J. Ehrhardt for his expertise in XPS analysis and J.M. Génin for his encouragement.

References

- [1] C. Frondel, *Am. Mineral.* 26 (1941) 295–315.
- [2] R. Allmann, *Acta Crystallogr. B* 24 (1968) 972–977.
- [3] F. Trolard, J.M.R. Génin, M. Abdelmoula, G. Bourrié, B. Humbertand, A. Herbillon, *Geochim. Cosmochim. Acta* 61 (1997) 1107–1111.
- [4] J.M.R. Génin, G. Bourrié, F. Trolard, M. Abdelmoula, A. Jaffrezic, Ph. Refait, V. Maître, B. Humbert, A. Herbillon, *Environ. Sci. Technol.* 32 (1998) 1058–1068.
- [5] P. Refait, M. Abdelmoula, F. Trolard, J.M.R. Génin, J.J. Ehrhardt, G. Bourrié, *Am. Mineral.* 86 (2001) 731–739.
- [6] A. de Roy, C. Forano, J.P. Besse, in: *Layered Double Hydroxides*, Nova Science Publishers, 2001, p. 1.
- [7] H.C.B. Hansen, in: *Layered Double Hydroxides*, Nova Science Publishers, 2001, p. 229.
- [8] M. Vucelic, W. Jones, G.D. Moggridge, *Clays Clay Miner.* 45 (1997) 803–813.
- [9] J.M.R. Génin, R. Aïssa, A. Géhin, M. Abdelmoula, O. Benali, V. Ernsten, G. Ona-Nguema, C. Upadhyay, C. Ruby, *Solid State Sci.* 7 (2005) 545–572.
- [10] Ph. Refait, O. Benali, M. Abdelmoula, J.M.R. Génin, *Corros. Sci.* 45 (2003) 2435–2449.
- [11] L. Legrand, L. Mazerolles, A. Chaussé, *Geochim. Cosmochim. Acta* 68 (2004) 3497–3507.
- [12] S. Peulon, H. Antony, L. Legrand, A. Chausse, *Electrochim. Acta* 49 (2004) 2891–2899.
- [13] C. Ruby, C. Upadhyay, A. Géhin, G. Ona-Nguema, J.M.R. Génin, *Environ. Sci. Technol.* 40 (2006) 4696–4702.
- [14] J.M.R. Génin, C. Ruby, C. Upadhyay, *Solid State Sci.* 8 (2006) 1330–1343.
- [15] H.C.B. Hansen, C.B. Koch, *Appl. Clay Sci.* 10 (1995) 5–19.
- [16] A.P. Grosvenor, B.A. Kobe, M.C. Biesinger, N.S. McIntyre, *Surf. Interf. Anal.* 36 (2004) 1564–1574.
- [17] F. Bocher, A. Géhin, C. Ruby, J. Ghanbaja, M. Abdelmoula, J.M.R. Génin, *Solid State Sci.* 6 (2004) 117–124.
- [18] P.C.J. Graat, M.A.J. Somers, E.J. Mittemeijer, *Appl. Surf. Sci.* (1998) 238–259.
- [19] R.P. Gupta, S.K. Sen, *Phys. Rev. B* 12 (1975) 15–19.
- [20] W. Temesghen, P.M.A. Sherwood, *Anal. Bioanal. Chem.* 373 (2002) 601–608.
- [21] A.P. Grosvenor, B.A. Kobe, N.S. McIntyre, *Surf. Sci.* 572 (2004) 217–227.
- [22] R.J. Lad, V.E. Henrich, *Phys. Rev. B* 39 (1989) 13478–13485.
- [23] L. Legrand, A. El Figuigui, F. Mercier, A. Chausse, *Environ. Sci. Technol.* 38 (2004) 4587–4595.
- [24] R.A. Maithreepala, R. Doong, *Environ. Sci. Technol.* 39 (2005) 4082–4090.
- [25] L.L. Skovbjerg, S.L.S. Stipp, S. Utsunomiya, R.C. Ewing, *Geochim. Cosmochim. Acta* 70 (2006) 3582–3592.
- [26] H.C.B. Hansen, C.B. Koch, H.N. Krogh, O.K. Borggaard, J. Sørensen, *Environ. Sci. Technol.* (1996) 2053–2056.